Structure and Chemical Properties of Chlorohydrido(diarylsilyl)rhodium(III) Complexes, *mer*-RhCl(H)($SiHAr_2$)(PMe_3)$_3$. Thermally Induced Chloro Transfer from Rhodium to Silicon in the Complexes and Silane Exchange

Kohtaro Osakada,* Susumu Sarai, Take-aki Koizumi, and Takakazu Yamamoto*

Research Laboratory of Resources Utilization, Tokyo Institute of Technology, 4259 Nagatsuta, Midori-ku, Yokohama 226, Japan

Received May 12, 1997[⊗]

Reactions of the diarylsilanes H_2SiPh_2, $H_2Si(C_6H_4Me\text{-}p)_2$, $H_2Si(C_6H_4OMe\text{-}p)_2$, $H_2Si(C_6H_4F\text{-}p)_2$, and $H_2Si(C_6H_4CF_3\text{-}p)_2$ with $[Rh(PMe_3)_4]Cl$ involve oxidative addition of an Si−H bond of the substrates to give *mer*-$RhCl(H)[SiH(C_6H_4X\text{-}p)_2](PMe_3)_3$ (**1**, X = H; **2**, X = Me; **3**, X = OMe; **4**, X = F; **5**, X = CF_3). X-ray crystallography of **1**, **3**, **4**, and **5** shows a distorted-octahedral coordination around the Rh center with three meridional PMe_3 ligands and with the chloro and diarylsilyl ligands at mutually trans positions. The Rh−Si bond distances of the complexes are in the range 2.311−2.319 Å. Addition of $H_2Si(C_6H_4Me\text{-}p)_2$ to a toluene solution of **1** results in partial conversion of the complex into **2** accompanied by liberation of H_2SiPh_2. The exchange of the diphenylsilyl ligand of **1** on addition of the other diarylsilanes proceeds reversibly at 10−50 °C with the thermodynamic parameters of the reactions **1** + $H_2Si(C_6H_4X\text{-}p)_2$ = *mer*-$RhCl(H)[SiH(C_6H_4X\text{-}p)_2](PMe_3)_3$ + H_2SiPh_2 as $\Delta H° = 4.16$ kJ mol^{-1} and $\Delta S° = 8.2$ J mol^{-1} K^{-1} for X = Me, $\Delta H° = 6.51$ kJ mol^{-1} and $\Delta S° = 11.7$ J mol^{-1} K^{-1} for X = OMe, and $\Delta H° = -2.33$ kJ mol^{-1} and $\Delta S° = -5.3$ J mol^{-1} K^{-1} for X = F, respectively. Enthalpy of the reactions of **1** with $H_2Si(C_6H_4X\text{-}p)_2$ (X = Me, OMe, and F) decreases with increase in the σ_p value of X. Heating a toluene solution of **1** at 50 °C and at 110 °C gives mixtures of *fac*-$Rh(H)_2(SiClPh_2)(PMe_3)_3$ (**6**) and $RhCl(H)(SiClPh_2)(PMe_3)_3$ (**7**). The structure of **6** has been determined by X-ray crystallography, while **7** was characterized by comparison of the NMR (^1H, $^{31}P\{^1H\}$, $^{13}C\{^1H\}$, and $^{29}Si\{^1H\}$) peaks with those of the complex prepared independently from the reaction of $HSiClPh_2$ with $[Rh(PMe_3)_4]Cl$.

Introduction

The structure and chemical properties of complexes containing Rh−Si bonds are of current interest[1] in relation to the mechanisms of Rh complex catalyzed reactions such as hydrosilylation,[2] silylformylation,[3] and dehydrogenative condensation of SiH and EH groups (E = O, N, S)[4] because these reactions are believed to involve silylrhodium complexes as the intermediates. There seems to be, however, several unclarified issues on the above catalytic reactions. For example, a detailed process for the formation of active species from added transition-metal complexes has not been revealed well in most cases.

H_2PtCl_6 is believed to react with organosilanes to generate Pt(0) species which act as the active species in the catalytic hydrosilylation. Dichloroplatinum(II) complexes as well as $IrCl(CO)(PPh_3)_2$ react with triorganosilanes to give active hydrido complexes of these elements and chlorotriorganosilanes.[5] $RhClL_n$ is also

[⊗] Abstract published in *Advance ACS Abstracts,* August 15, 1997.

(1) Reviews and recent articles: (a) Tilley, T. D. Transition-metal Silyl Derivatives In *The Chemistry of Organic Silicon Compounds*; Patai, S., Rappoport, Z., Eds.; Wiley: New York, 1989; p 1415. (b) Hendriksen, D. E.; Oswald, A. A.; Ansell, G. B.; Leta, S.; Kastrup, R. V. *Organometallics* **1989**, *8*, 1153. (c) Joslin, F. L.; Stobart, S. R. *J. Chem. Soc., Chem. Commun.* **1989**, 504. (d) Thorn, D. L.; Harlow, R. L. *Inorg. Chem.* **1990**, *29*, 2017. (e) Wang, W.-D.; Eisenberg, R. *J. Am. Chem. Soc.* **1990**, *112*, 1833. (f) Fryzuk, M. D.; Rosenberg, L.; Rettig, S. J. *Organometallics* **1991**, *10*, 2537. (g) Osakada, K.; Hataya, K.; Nakamura, Y.; Tanaka, M.; Yamamoto, T. *J. Chem. Soc., Chem. Commun.* **1993**, 576. (h) Osakada, K.; Hataya, K.; Yamamoto, T. *J. Chem. Soc., Chem. Commun.* **1995**, 2315. (i) Osakada, K.; Hataya, K.; Yamamoto, T. *Inorg. Chim. Acta* in press. (j) Osakada, K.; Koizumi, T.; Yamamoto, T. *Bull. Chem. Soc. Jpn.* **1997**, *70*, 189. (k) Osakada, K.; Koizumi, T.; Yamamoto, T. *Organometallics* **1997**, *16*, 2093. (l) Nagashima, H.; Tatebe, K.; Ishibashi, T.; Nakaoka, A.; Sakakibara, J.; Itoh, K. *Organometallics* **1995**, *14*, 2868. (m) Hofmann, P.; Meier, C.; Hiller, W.; Heckel, M.; Riede, J.; Schmidt, M. U. *J. Organomet. Chem.* **1995**, *490*, 51. (n) Marciniec, B.; Krzyzanowski, P. *J. Organomet. Chem.* **1995**, *493*, 261. (o) Aizenberg, M.; Goikhman, R.; Milstein, D. *Organometallics* **1996**, *15*, 1075.

(2) (a) Ojima, I. In *Organic Transition-Metal Chemistry*; Ishii, Y., Tsutsui, M., Eds.; Plenum: New York, 1975; p 255. (b) Speier, J. L. Homogeneous Catalysis of Hydrosilation by Transition Metals. *Adv. Organomet. Chem.* **1979**, *17*, 407. (c) Jardin, F. H. In *The Chemistry of the Metal Carbon Bond*; Hartley, F. R., Ed.; Wiley: New York, 1987; Vol. 4, (Organometallic Compounds in Organic Synthesis), p 784. (d) Ojima, I. The Hydrosilylation Reaction. In *The Chemistry of Organic Silicon Compounds*; Patai, S., Rappoport, Z., Eds.; Wiley: New York, 1989; p 1479.

(3) (a) Matsuda, I.; Ogiso, A.; Sato, S.; Izumi, Y. *J. Am. Chem. Soc.* **1989**, *111*, 2332. (b) Matsuda, I.; Ogiso, A.; Sato, S. *J. Am. Chem. Soc.* **1990**, *112*, 6120. (c) Ojima, I.; Ingallina, P.; Donovan, R. J.; Clos, N. *Organometallics* **1990**, *10*, 38.

(4) (a) Ojima, I.; Inaba, S.; Kogure, T.; Nagai, Y. *J. Organomet. Chem.* **1973**, *55*, C7. (b) Lappert, M. F.; Maskell, R. K. *J. Organomet. Chem.* **1984**, *264*, 217. (c) Seyferth, D.; Wiseman, G. H. *J. Am. Ceram. Soc.* **1984**, *67*, C132. (d) Blum, Y.; Laine, R. M. *Organometallics* **1986**, *5*, 2081. (e) Corey, J. Y.; Chang, L. S.; Corey, E. R. *Organometallics* **1987**, *6*, 1595. (f) Chang, L. S.; Corey, J. Y. *Organometallics* **1989**, *8*, 1885. (g) Choong Kwet Yive, N. S.; Corriu, R. J. P.; Leclericq, D.; Mutin, H.; Vioux, A. *Chem. Mater.* **1992**, *4*, 141. (h) Liu, H. Q.; Harrod, J. F. *Organometallics* **1992**, *11*, 822. (i) He, J.; Liu, H. Q.; Harrod, J. F.; Hynes, R. *Organometallics* **1994**, *13*, 336. (j) Baruah, J. B.; Osakada, K.; Yamamoto, T. *J. Mol. Catal.* **1995**, *101*, 17. (k) Baruah, J. B.; Osakada, K.; Yamamoto, T. *Organometallics* **1996**, *15*, 456.

S0276-7333(97)00391-9 CCC: $14.00

Table 1. Yields, Analytical Results, and IR Data of Complexes 1−7

complex	yield (%)[a]	anal. (%) C[b]	anal. (%) H[b]	IR data ν(RhH)[c]	IR data ν(SiH)[c]
mer-RhCl(H)($SiHPh_2$)(PMe_3)$_3$ (**1**)	96	45.78 (45.78)	7.19 (7.14)	1944	2054
mer-RhCl(H)[$SiH(C_6H_4Me$-*p*$)_2$](PMe_3)$_3$ (**2**)	87	47.41 (47.72)	7.70 (7.49)	1970	2064
mer-RhCl(H)[$SiH(C_6H_4OMe$-*p*$)_2$](PMe_3)$_3$ (**3**)	81	45.38 (45.22)	7.05 (7.09)	2014	2030
mer-RhCl(H)[$SiH(C_6H_4F$-*p*$)_2$](PMe_3)$_3$ (**4**)	94	43.13 (42.98)	6.70 (6.35)	1952	2056
mer-RhCl(H)[$SiH(C_6H_4CF_3$-*p*$)_2$](PMe_3)$_3$ (**5**)	88	40.12 (40.22)	5.95 (5.43)	1956	2054
fac-Rh(H)$_2$($SiClPh_2$)(PMe_3)$_3$ (**6**)[d]	36	45.65 (45.78)	7.04 (7.14)		
mer-RhCl(H)($SiClPh_2$)(PMe_3)$_3$ (**7**)[e]	70	42.57 (43.09)	6.54 (6.54)		

[a] Yields shown are before recrystallization, but their purity is confirmed by ^{1}H and ^{31}P{^{1}H} NMR spectra. [b] Calculated values are in parentheses. [c] In cm^{-1} as KBr disks. [d] Yield from the thermal reaction of **1**: Cl, 6.30 (6.44). [e] Yield from the reaction of [Rh(PMe_3)$_4$]Cl with $HSiClPh_2$: Cl, 12.02 (12.11).

Scheme 1

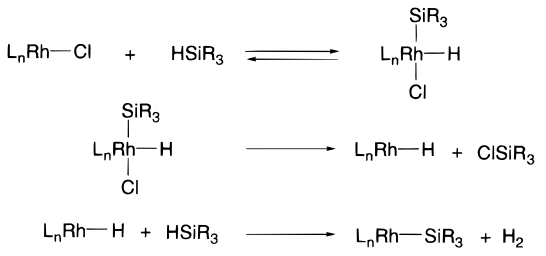

Scheme 2

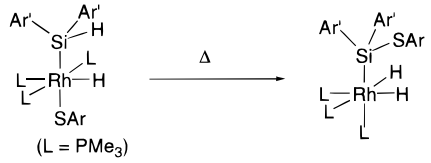

expected to undergo removal of the chloro ligand as chloroorganosilanes in the reactions with organosilanes to leave the hydrido- or silylrhodium(I) complexes as the product. Reactions of triarylsilanes with RhCl(P(*i*-Pr)$_3$)$_2$ actually cause liberation of chloroorganosilanes; however, the produced hydridorhodium species are trapped by another rhodium complex to form bimetallic rhodium products such as (P(*i*-Pr)$_3$)(Ar$_3$Si)HRh(μ-H)(μ-Cl)RhH(SiAr$_3$)(P(*i*-Pr)$_3$).[1j,k] These reactions are considered to proceed through oxidative addition of the Si−H bond to the Rh(I) center followed by reductive elimination of chloroorganosilane from the resulting Rh(III) species as depicted in Scheme 1. Details of this type of the reaction, however, have not been investigated well.

On the other hand, we have recently reported that *mer*-RhH(SAr)($SiHAr'_2$)(PMe_3)$_3$ undergoes thermally induced transfer of the thiolato ligand to give *fac*-Rh(H)$_2$[Si(SAr)Ar′$_2$](PMe_3)$_3$, as shown in Scheme 2.[1h] A similar transfer of the chloro ligand of an analogous complex, *mer*-RhCl(H)($SiHPh_2$)(PMe_3)$_3$, if it occurs, is expected to provide a clue to elucidate the mechanism of generation of chloroorganosilane and the hydrido- or silylrhodium(I) complex from the reaction of a chlororhodium(I) complex and organosilane. In this paper we report the preparation and such a chloro ligand transfer reaction of *mer*-RhCl(H)($SiHAr_2$)(PMe_3)$_3$ type complexes as well as results from thermodynamic measurement of the reaction of the complexes with diarylsilanes.

(5) (a) Chalk, A. J. *J. Chem. Soc., Chem. Commun.* **1969**, 1207. (b) Chalk, A. J.; Harrod, J. F. *J. Am. Chem. Soc.* **1965**, *87*, 16. (c) Cundy, C. S.; Kingston, B. M.; Lappert, M. F. *Adv. Organomet. Chem.* **1973**, *11*, 253.

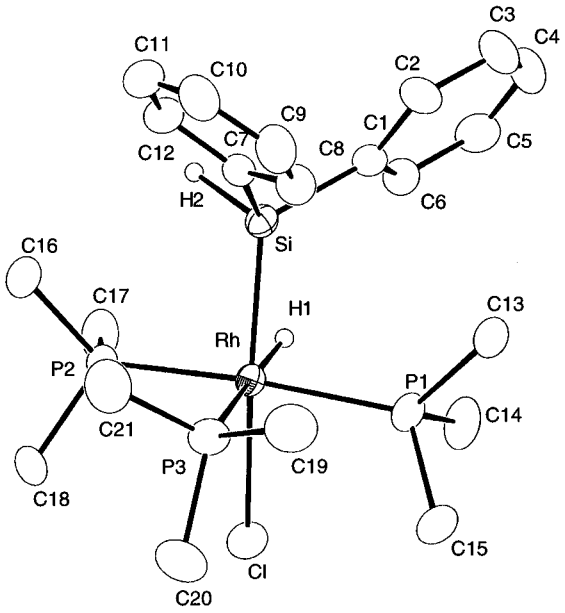

Figure 1. ORTEP drawing of *mer*-RhCl(H)($SiHPh_2$)(PMe_3)$_3$ (**1**) at the 30% ellipsoid level. Hydrogen atoms except for the RhH and SiH hydrogens are omitted for simplicity.

Results and Discussion

Preparation and Characterization of *mer*-RhCl(H)($SiHAr_2$)(PMe_3)$_3$ (1−5). A Rh(I) complex with PMe_3 ligands, [Rh(PMe_3)$_4$]Cl, readily reacts with an equimolar or slightly excess amount of $H_2Si(C_6H_4X$-*p*$)_2$ to give *mer*-RhCl(H)[$SiH(C_6H_4X$-*p*$)_2$](PMe_3)$_3$ (**1**, X = H; **2**, X = Me; **3**, X = OMe; **4**, X = F; **5**, X = CF_3) as shown in eq 1. Table 1 summarizes yields, analytical

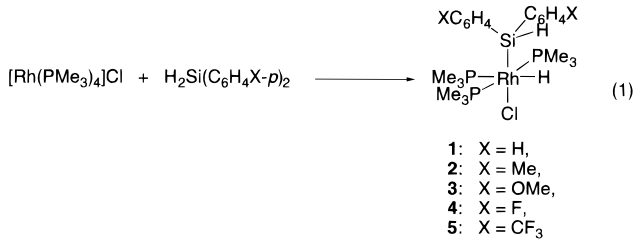

results, and selected IR data. The complexes are isolated in high yields and give rise to characteristic IR peaks due to ν(RhH) and ν(SiH) vibrations at reasonable positions. Figures 1−4 show molecular structures of **1**, **3**, **4**, and **5** determined by X-ray crystallography. Each molecule has a distorted-octahedral coordination around the Rh center with three PMe_3 ligands at meridional coordination sites. The chloro and diarylsilyl ligands

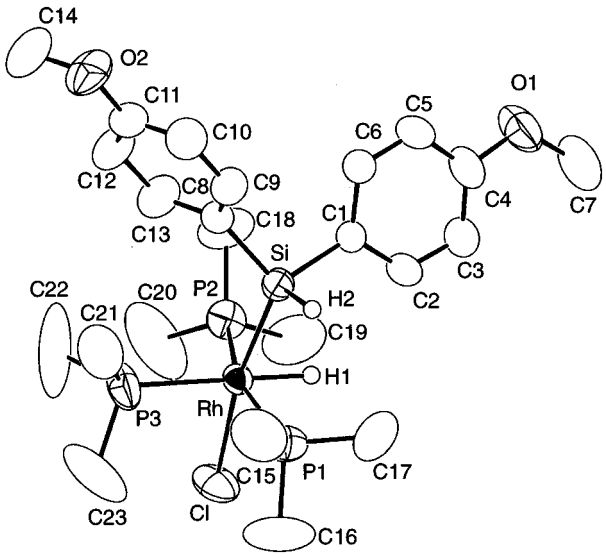

Figure 2. ORTEP drawing of *mer*-RhCl(H)(SiH(C_6H_4OMe-*p*)$_2$)(PMe_3)$_3$ (**3**) at the 30% ellipsoid level. Hydrogen atoms except for the RhH and SiH hydrogens are omitted for simplicity.

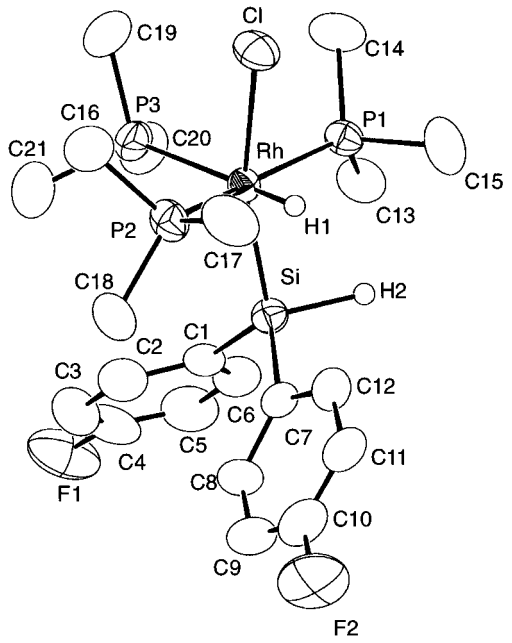

Figure 3. ORTEP drawing of *mer*-RhCl(H)(SiH(C_6H_4F-*p*)$_2$)(PMe_3)$_3$ (**4**) at the 30% ellipsoid level. Hydrogen atoms except for RhH and SiH hydrogens are omitted for simplicity.

are situated at mutually trans positions. The coordination around the Rh center of **1**−**5** is quite similar to that of the thiolato analogues, *mer*-RhH(SAr)(SiHAr′$_2$)(PMe_3)$_3$ and *mer*-RhH(SAr)($SiPh_3$)(PMe_3)$_3$, which also possess the thiolato and di- or triarylsilyl ligands at mutually trans positions.[1h,i] Table 2 summarizes selected bond distances and angles around the Rh center. Rh−P3 bonds of the complexes are longer than Rh−P1 and Rh−P2 bonds due to a large trans influence of the hydrido ligand. The greater bulk of the PMe_3 ligand in comparison to the hydride renders P1−Rh−P3 and P2−Rh−P3 bond angles larger than 90°. Rh−Si bond distances of the complexes are in the range 2.311−2.319 Å, whose variance falls within the standard deviations.

The NMR data (^{1}H and ^{31}P{^{1}H}) of **1**−**5**, summarized in Table 3, as well as results of ^{13}C{^{1}H} and ^{29}Si{^{1}H}

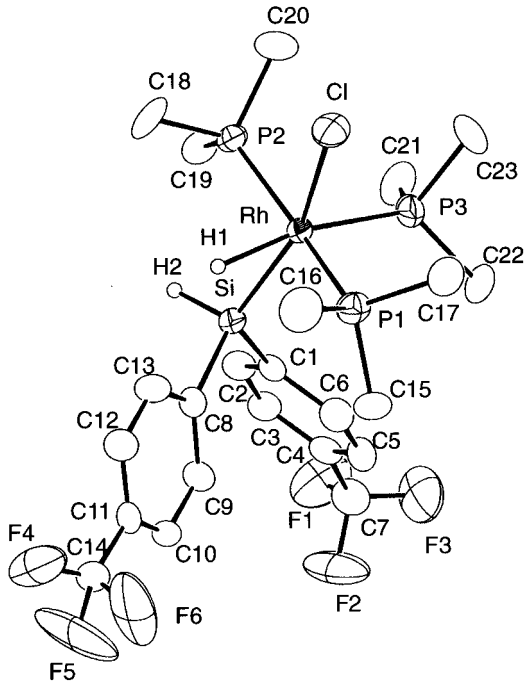

Figure 4. ORTEP drawing of *mer*-RhCl(H)(SiH($C_6H_4CF_3$-*p*)$_2$)(PMe_3)$_3$ (**5**) at the 30% ellipsoid level. Hydrogen atoms except for the RhH and SiH hydrogens are omitted for simplicity.

Table 2. Selected Bond Distances (Å) and Angles (deg) for 1, 3, 4, and 5

	1	3	4	5
Rh−Cl	2.545(4)	2.540(2)	2.549(2)	2.521(3)
Rh−P1	2.326(4)	2.325(2)	2.315(2)	2.317(3)
Rh−P2	2.316(4)	2.327(1)	2.336(2)	2.317(3)
Rh−P3	2.378(4)	2.394(2)	2.368(2)	2.378(5)
Rh−Si	2.313(4)	2.319(2)	2.311(2)	2.312(3)
Cl−Rh−P1	83.4(1)	91.69(6)	87.28(6)	83.2(1)
Cl−Rh−P2	86.8(1)	84.83(5)	82.15(7)	85.3(1)
Cl−Rh−P3	93.6(1)	88.92(7)	93.29(7)	94.3(1)
P1−Rh−P2	164.5(1)	160.84(6)	163.86(7)	164.3(1)
P2−Rh−P3	96.4(1)	102.94(5)	96.58(7)	94.9(1)
P1−Rh−P3	96.2(1)	95.81(6)	96.17(7)	96.5(1)
Si−Rh−Cl	162.1(1)	169.35(4)	161.88(6)	159.3(2)
Si−Rh−P1	96.8(1)	86.29(6)	88.86(6)	97.1(1)
Si−Rh−P2	89.0(1)	93.66(5)	97.41(7)	90.0(1)
Si−Rh−P3	104.1(1)	101.68(7)	104.72(7)	106.2(1)

NMR measurements are consistent with the above structures found by crystallography. The ^{1}H and ^{13}C{^{1}H} NMR spectra show the signals due to PMe_3 at mutually trans positions and that bonded trans to the hydrido ligand. The former signals appear as an apparent triplet arising from virtual coupling, while the latter is observed as a simple doublet. The ^{1}H signal due to the hydride shows splitting due to coupling with the P nucleus at a trans position (166−167 Hz) and due to coupling with the other P and Rh nuclei (13−19 Hz). The SiH hydrogen signals appear at δ 5.10−5.35 accompanied by coupling with Rh and P nuclei (10−12 Hz). The ^{31}P{^{1}H} NMR spectra of **1**−**5** show a doublet of doublets and a doublet of triplets, which are assigned to the two PMe_3 ligands at mutually trans positions and a PMe_3 trans to the hydride, respectively. The ^{29}Si{^{1}H} NMR signal of **1** appears at δ 14.9 accompanied by splitting due to J(SiRh) (43 Hz) and J(SiP) (8 and 7 Hz) coupling. The similarity of the J(SiP) values is consistent with the structure having all three PMe_3 ligands

Table 3. NMR Data (ppm) for Complexes 1−7

	^{1}H NMR[a]			^{31}P{^{1}H} NMR[b]
	Rh−H	$P(CH_3)_3$	other	
1	−8.85 (ddt, 1H, *J*(RhH) = 15 Hz, *J*(PH) = 167 and 18 Hz)	1.01 (d, 9H, *J* = 7 Hz) 1.27 (18H)[c]	5.30 (dt, 1H, SiH, *J* = 10,10,12 Hz)	−9.0 (dd, *J*(RhP) = 100 Hz, *J*(PP) = 31 Hz) −25.3 (dt, *J*(RhP) = 90 Hz)
2	−8.78 (ddt, 1H, *J*(RhH) = 16 Hz, *J*(PH) = 167 and 18 Hz)	1.06 (d, 9H, *J* = 7 Hz) 1.31 (18H)[c]	5.34 (dt, 1H, SiH, *J* = 10,10,12 Hz) 2.14 (s, 6H, CH_3)	−8.9 (dd, *J*(RhP) = 102 Hz, *J*(PP) = 31 Hz) −25.1 (dt, *J*(RhP) = 90 Hz)
3	−8.80 (ddt, 1H, *J*(RhH) = 15 Hz, *J*(PH) = 167 and 18 Hz)	1.06 (d, 9H, *J* = 7 Hz 1.32 (18H)[c]	5.35 (dt, 1H, SiH, *J* = 10,10,12 Hz) 3.33 (s, 6H, OCH_3)	−8.7 (dd, *J*(RhP) = 101 Hz, *J*(PP) = 31 Hz) −25.0 (dt, *J*(RhP) = 94 Hz)
4	−8.99 (ddt, 1H, *J*(RhH) = 15 Hz, *J*(PH) = 166 and 18 Hz)	0.97 (d, 9H, *J* = 6 Hz) 1.20 (18H)[c]	5.16 (dt, 1H, SiH, *J* = 10,10,12 Hz)	−9.2 (dd, *J*(RhP) = 98 Hz, *J*(PP) = 31 Hz) −25.5 (dt, *J*(RhP) = 94 Hz)
5	−9.00 (ddt, 1H, *J*(RhH) = 13 Hz, *J*(PH) = 167 and 19 Hz)	0.93 (d, 9H, *J* = 7 Hz) 1.13 (18H)[c]	5.10 (dt, 1H, SiH, *J* = 10,10,12 Hz)	−9.5 (dd, *J*(RhP) = 98 Hz, *J*(PP) = 31 Hz) −25.6 (dt, *J*(RhP) = 94 Hz)
6	−10.04 (m, 2H, *J*(PH) = 117 Hz)	1.02 (d, 18H, *J* = 6 Hz) 1.07 (d, 9H, *J* = 6 Hz)		−16.7 (dd, *J*(RhP) = 100 Hz, *J*(PP) = 25 Hz) −23.4 (dt, *J*(RhP) = 90 Hz)
7	−8.78 (ddt, 1H, *J*(RhH) = 15 Hz, *J*(PH) = 161 and 18 Hz)	1.25 (d, 9H, *J* = 7 Hz) 1.13 (18H)[c]		−8.7 (dd, *J*(RhP) = 93 Hz, *J*(PP) = 35 Hz) −22.4 (dt, *J*(RhP) = 94 Hz)

[a] 400 MHz at 25 °C in C_6D_6. [b] 160 MHz at 25 °C in C_6D_6. Chemical shifts are referenced to external 85% H_3PO_4. [c] Apparent triplet due to virtual coupling.

Scheme 3

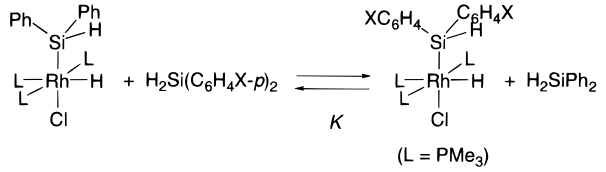

Table 4. Equilibrium Constants of Reaction of 1 with $H_2Si(C_6H_4X\text{-}p)_2$ in Scheme 3

	K[a]		
temp (K)	X = Me	X = OMe	X = F
283		0.256	1.420
288	0.474		
293		0.284	1.350
298	0.501		
303		0.305	1.330
308	0.527		
313		0.336	1.290
318	0.559		
323		0.362	

[a] $K = [H_2SiPh_2][RhCl(H)\{SiH(C_6H_4X)_2\}(PMe_3)_3][H_2Si(C_6H_4X)_2]^{-1}[\mathbf{1}]^{-1}$.

at cis positions with regard to the diphenylsilyl ligand in the molecule.

Thermodynamic Measurement on Exchange of the Diphenylsilyl Ligand on Addition of Diarylsilanes. Addition of $H_2Si(C_6H_4Me\text{-}p)_2$ to a toluene solution of **1** causes partial conversion of the complex into **2** accompanied by liberation of H_2SiPh_2. The ^{1}H NMR spectra of solutions containing **1**, **2**, H_2SiPh_2, and $H_2Si(C_6H_4X\text{-}p)_2$ (X = Me, OMe, and F) show reversible and rapid exchange between the diarylsilyl and hydrido ligands on the Rh center and diarylsilanes in the solution, indicating the presence of the equilibrium shown in Scheme 3. The equilibrium constants are obtained by comparison of the ^{1}H NMR peak area ratios (SiH and $P(CH_3)_3$ regions) of the mixtures in the temperature range 10−50 °C and are summarized in Table 4. The temperature dependence of the equilibrium constants shown in Figure 5 gives the thermodynamic parameters of the reactions $\Delta H° = 4.16$ kJ mol^{-1} and $\Delta S° = 8.2$ J mol^{-1} K^{-1} for X = Me, $\Delta H° = 6.51$ kJ mol^{-1} and $\Delta S° = 11.7$ J mol^{-1} K^{-1} for X = OMe, and $\Delta H° = -2.33$ kJ mol^{-1} and $\Delta S° = -5.3$ J mol^{-1} K^{-1} for X = F, respectively, at 298 K. The reaction enthalpy

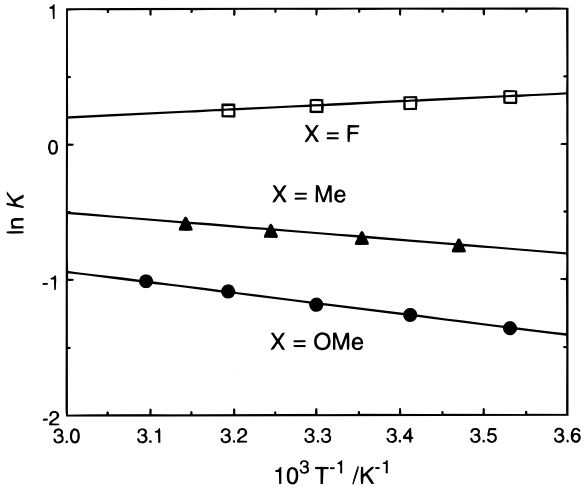

Figure 5. van't Hoff plots of the reaction of **1** with diarylsilanes.

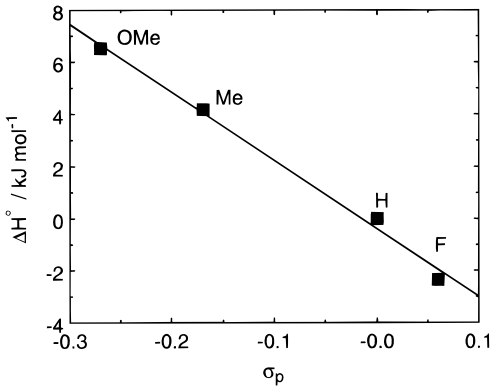

Figure 6. Hammett plot of the enthalpy of the reaction in Scheme 3.

varies depending on the substituent X of the diarylsilyl ligand. Figure 6 shows a linear relationship between the σ_p and $\Delta H°$ values of the reactions for X = H, Me, OMe, F. The negative ρ value of the plots suggests that a more electron-withdrawing substituent on the diarylsilyl group stabilizes the Rh−Si bond of the complex and/or destabilizes the Si−H bond of the diarylsilane more significantly.

D(Si−H) values for $MeSiH_3$ and $PhSiH_3$ have been determined as 375 and 369 kJ mol^{-1}, respectively;[6] the

Scheme 4

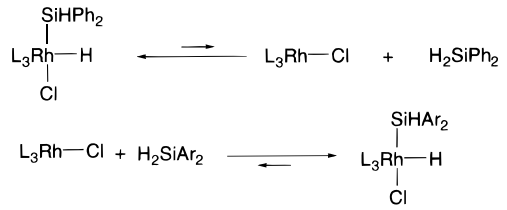

difference in the dissociation energy of the Si−H bond when the substituent on the Si center is changed is, therefore, considered to be not large. Variance of D(Si−H) values for $H_2Si(C_6H_4X\text{-}p)_2$ (X = OMe, Me, H, and F) should be even smaller because the effect of X-*p* is less direct. The $\Delta H°$ values of the above reactions ranging from −2.3 to 4.2 kJ mol^{-1} seem to be governed by the difference in D(Rh−Si) depending on X rather than that of D(Si−H). Thus, a diarylsilyl group with a more electron-withdrawing substituent on the phenyl ring forms a more stable Rh−Si bond, which contributes to shift the above equilibrium to the right.

Scheme 4 depicts a plausible pathway of the reaction of **1** with diarylsilane. Reductive elimination of diphenylsilane from **1** followed by immediate oxidative addition of diarylsilane to the resulting $RhCl(PMe_3)_3$ accounts for the reversible exchange of the organosilyl ligands. The above mechanism is more plausible than an alternative mechanism involving σ-bond metathesis reaction of the Si−H and Rh−Si bonds because an equimolar reaction of **3** with D_2SiPh_2 gives a mixture of the non-deuterated complex **3**, *mer*-RhCl(D)(SiDPh$_2$)(PMe$_3$)$_3$ (**1**-d_2), $H_2Si(C_6H_4OMe\text{-}p)_2$, and D_2SiPh_2 and does not give $HDSiPh_2$ (or H_2SiPh_2) nor **3**-d (or **3**-d_2).[7]

The reductive elimination of the diarylsilane in Scheme 4 is not thermodynamically favored because the NMR spectra of **1**−**5** do not show the signals due to the liberated diarylsilane and because the $^{29}Si\{^1H\}$ NMR peak of **1** shows coupling with Rh and P nuclei. Similar complexes with a thiolato ligand, *mer*-Rh(SAr)H(SiHAr$_2$)(PMe$_3$)$_3$, do not show evidence for the reductive elimination of diarylsilane, while a complex with an $SiPh_3$ ligand, *mer*-Rh(SPh)H(SiPh$_3$)(PMe$_3$)$_3$, readily liberates $HSiPh_3$ at room temperature to give an equilibrated mixture of *mer*-Rh(SPh)H(SiPh$_3$)(PMe$_3$)$_3$, Rh(SPh)(PMe$_3$)$_3$, and $HSiPh_3$.[1i]

Thermally Induced Chloro Ligand Transfer Reaction. Heating a toluene solution of **1** for 90 min at 110 °C results in transformation of the complex into a mixture of *fac*-Rh(H)$_2$(SiClPh$_2$)(PMe$_3$)$_3$ (**6**) and *mer*-RhCl(H)(SiClPh$_2$)(PMe$_3$)$_3$ (**7**) in a 88:12 molar ratio as shown in eq 2. Complex **6** is isolated by fractional crystallization of the reaction product and characterized by X-ray crystallography and NMR analyses. Figure 7 shows the molecular structure with a distorted-octahedral coordination around the Rh center. Three P−Rh−P angles as well as Si−Rh−P1 and Si−Rh−P2 angles are considerably larger than 90°, owing to severe congestion among PMe_3 and $SiClPh_2$ ligands. The ^1H

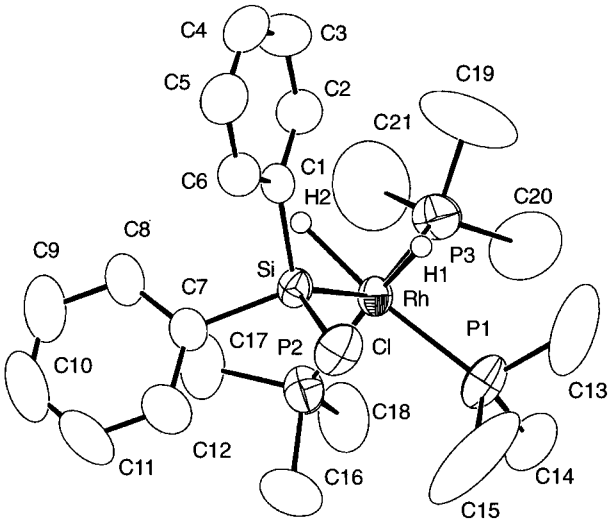

Figure 7. ORTEP drawing of *fac*-Rh(H)$_2$(SiClPh$_2$)(PMe$_3$)$_3$ (**6**) at the 30% ellipsoid level. Hydrogen atoms except for the RhH hydrogens are omitted for simplicity. Selected bond distances (Å) and angles (deg): Rh−P1, 2.324(2); Rh−P2, 2.332(2); Rh−P3, 2.344(2); Rh−Si, 2.314(2), Rh−H1, 1.42; Rh−H2, 1.75; Si−Cl, 2.163(2); P1−Rh−P2, 95.91(6); P1−Rh−P3, 98.93(6); P2−Rh−P3, 100.71(6); P1−Rh−Si, 107.68(6); P2−Rh−Si, 101.80(5); P3−Rh−Si, 142.84(6); Rh−Si−Cl, 116.74(7).

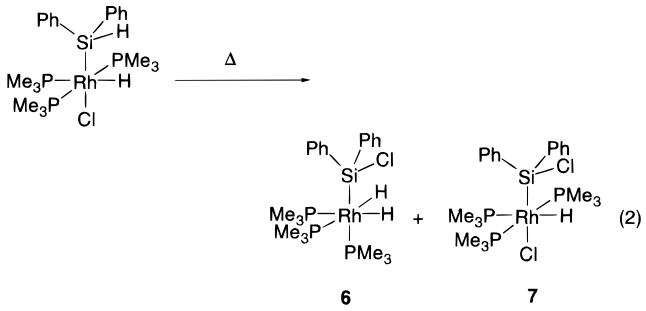

NMR spectrum of **6** shows complicated hydrido signals due to a second-order spin system. The peak pattern is quite similar to that of *fac*-Rh(H)$_2$[Si(SC$_6$H$_4$X-*p*)Ph$_2$](PMe$_3$)$_3$ (X = H, Me, OMe).[1h] The $^{29}Si\{^1H\}$ NMR peak at δ 51.6 shows splitting due to coupling with the trans P nucleus (198 Hz) and with Rh and the other P nuclei (41 and 11 Hz, respectively).

Another product of the reaction, **7**, is prepared independently by oxidative addition of $HClSiPh_2$ to $[Rh(PMe_3)_4]Cl$, as shown in eq 3. The NMR (^1H,

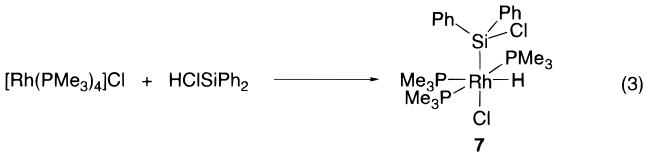

$^{31}P\{^1H\}$, and $^{29}Si\{^1H\}$) peaks of **7** isolated from reaction (3) agree well with those observed in the product of reaction (2) as a mixture with **6**. The ^1H and $^{31}P\{^1H\}$ NMR spectra of **7** show peaks quite similar to those of **1** except for the absence of ^1H NMR peaks due to an SiH hydrogen.

Reaction 2 for 17 days at 50 °C gives the products in a 64:36 molar ratio. Figure 8 shows a change in the ^1H NMR spectrum (hydrido region) during the reaction at that temperature. Both complexes **6** and **7** appear in

(6) (a) Walsh, R. Thermochemistry. In *The Chemistry of Organic Silicon Compounds*; Patai, S., Rappoport, Z., Eds.; Wiley: New York, 1989; p 384, and references therein. (b) Müller, U.; Popowski, E. *Z. Phys. Chem. (Leipzig)* **1990**, *271*, 703.

(7) After reaction for 1 h the ^1H NMR peaks due to **1**-*d*, **1**-d_0, H_2SiPh_2, and $HDSiPh_2$ were observed. This random scrambling of Si−H(D) and Rh−H(D) is slower than the silyl ligand exchange reaction in Scheme 3 and is not related to the process.

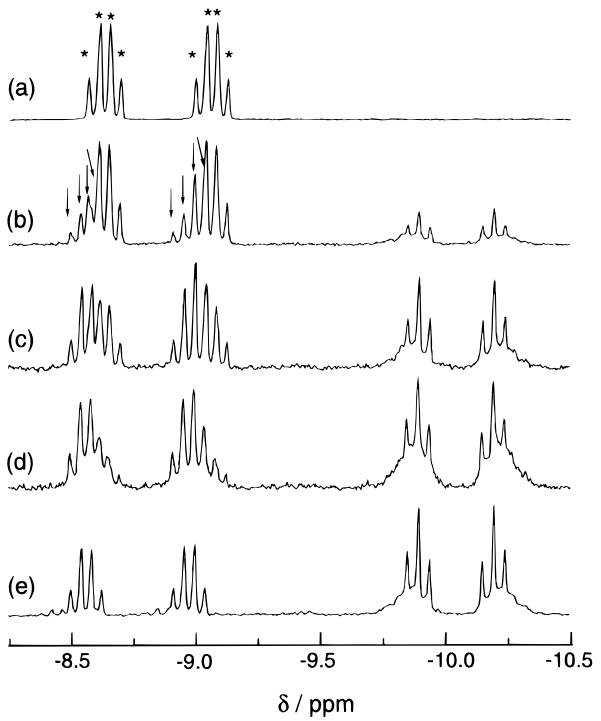

Figure 8. Change of the ^{1}H NMR spectrum (hydride region) during the thermal reaction of **1** giving a mixture of **6** and **7** after reaction for (a) 0 h, (b) 48 h, (c) 120 h, (d) 168 h, and (e) 400 h. Asterisks and arrows indicate positions of the hydrido peaks of **1** and **7**, respectively. These peaks are partly overlapped with each other throughout the reaction. The peaks around δ −10.0 are assigned to **6**, which show a complicated signal due to a second-order spin system.

the reaction mixture from the beginning and seem to increase at rates similar to each other. Formation of **7** from **1** should accompany other chlorine-free Rh-containing products, but NMR peaks due to these byproducts are not observed, possibly due to their extreme peak broadening or formation of uncharacterized paramagnetic complexes as the product. The presence of small amounts of organic compounds with an Si−H hydrogen is noticed in the ^{1}H NMR spectrum of the reaction mixture, but neither isolation nor characterization of the compounds is feasible.

Several related reactions have been examined in order to obtain more insight into the pathways of reaction 2. Heating a toluene solution of **6** at 80 °C leads to partial conversion of the complex into the isomer *cis,mer*-$Rh(H)_2(SiClPh_2)(PMe_3)_3$ (**8**), as shown in eq 4. The ^{1}H

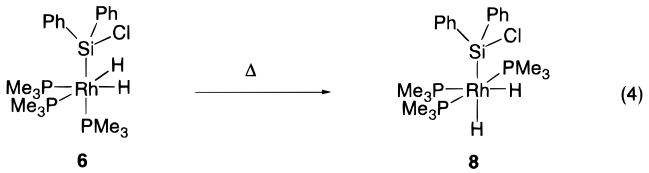

(4)

and $^{31}P\{^1H\}$ NMR spectra show the presence of only **6** and **8** in the reaction mixture, while isolation of the latter complex by fractional crystallization is not successful. The product of reaction 2 does not contain **8**, since conversion of **1** into a mixture of **6** and **7** is faster than thermal isomerization of **6** into **8**. Addition of $HClSiPh_2$ to a solution of **6** at room temperature or at elevated temperature gives **7**.

Formation of **6** in reaction 2 is easily interpreted by intramolecular or intermolecular exchange of the chloro ligand and SiH hydrogen accompanied by change of the sites of phosphine ligands, although the intramolecular exchange requires change in the coordination around Rh to situate the chloro and diphenylsilyl ligands at mutually cis positions prior to the Si−Cl bond formation. Complex **7** is formed through a more complicated route in the reaction and seems to involve an intermolecular process. Partial reductive elimination of $HSiClPh_2$ from once formed **6** and its ensuing oxidative addition to $[Rh(PMe_3)_4]Cl$ remaining intact in the reaction mixture would afford complex **7** according to reaction 3. Abstraction of chlorine of $HSiClPh_2$ promoted by **6** may also rationalize formation of **7**. At present we are not able to compare the possibility of these routes leading to **7** and to conclude whether **6** and **7** are formed independently or not because other products in the reaction mixture, including the NMR-inactive chlorine-free Rh complex, have not been characterized yet. Thiolato ligand transfer of *mer*-$RhH(SAr)(SiHAr'_2)(PMe_3)_3$ to give *fac*-$RhH_2[Si(SAr)Ar'_2](PMe_3)_3$ proceeds according to first-order kinetics with rate constants $(1.5-4.7) \times 10^{-4}$ s^{-1} at 40 °C, which corresponds to half-life times in the range 0.4−1.3 h at that temperature.[1h] Figure 8 suggests much longer half-life time for the conversion of **1** into a mixture of **6** and **7** even at 50 °C.[8] A much slower transfer of the chloro ligand of **1** to give **6** in comparison to the corresponding thiolato transfer of *mer*-$RhH(SAr)(SiHAr'_2)(PMe_3)_3$ seems to induce a side reaction to give **7**.

Conclusion

A series of *mer*-$RhCl(H)[SiH(C_6H_4X\text{-}p)_2](PMe_3)_3$ species have been prepared. Equilibrium measurement on the reaction of the complexes with diarylsilanes shows a tendency for the diarylsilyl group with a more electron-withdrawing substituent on the phenyl ring to stabilize the Rh−Si bonds to a greater extent. The reaction also suggests rapid reductive elimination of the diarylsilane followed by immediate reoxidative addition. The complexes undergo thermally induced chloro ligand transfer to give a mixture of *fac*-$Rh(H)_2(SiClPh_2)(PMe_3)_3$ and *mer*-$RhCl(H)(SiClPh_2)(PMe_3)_3$, the latter of which is formed through an intermolecular process. The results indicate that a chloro ligand bonded to the Rh center undergoes facile transfer onto the Si atom bonded to the metal center, even in the rigid octahedral coordination.

Experimental Section

General Considerations, Measurement, and Materials. Manipulations of the metal complexes were carried out under nitrogen or argon using standard Schlenk techniques. $[Rh(PMe_3)_4]Cl$, $H_2Si(C_6H_4Me\text{-}p)_2$, $H_2Si(C_6H_4OMe\text{-}p)_2$, $H_2Si(C_6H_4F\text{-}p)_2$, $H_2Si(C_6H_4CF_3\text{-}p)_2$, and D_2SiPh_2 were prepared

(8) The half-life time of reaction 2 is longer than 48 h at 50 °C, as judged from the peak area ratio of Figure 8. Measurement of the rate of conversion of **1** into a mixture of **6** and **7** is examined in the temperature range 75−100 °C. Time conversion curves suggest first-order kinetics with rate constants of 3.3×10^{-5}−2.1×10^{-4} s^{-1}, although the actual kinetic formula of the reaction giving two or more products is more complicated. Extrapolation of the Eyring plots gives rise to a rate constant on the basis of the assumption of first-order kinetics, 1.8×10^{-6} s^{-1} at 40 °C, that is much smaller than the thiolato ligand transfer in ref 1h.

Table 5. Crystal Data and Details of the Structure Refinement of 1, 3, 4, 5, and 6

	1	3	4	5	6
formula	$C_{21}H_{39}ClP_3RhSi$	$C_{23}H_{43}ClO_2P_3RhSi$	$C_{21}H_{37}ClF_2P_3RhSi$	$C_{23}H_{37}ClF_6P_3RhSi$	$C_{21}H_{39}ClP_3RhSi$
mol wt	550.90	610.96	586.89	686.90	550.90
cryst syst	orthorhombic	monoclinic	orthorhombic	monoclinic	orthorhombic
space group	*Fdd*2 (No. 43)	$P2_1/n$ (No. 14)	*Fdd*2 (No. 43)	*C*2/*c* (No. 15)	*Pbca* (No. 61)
a (Å)	27.359(4)	8.933(4)	27.383(10)	17.963(8)	20.343(9)
b (Å)	39.559(4)	12.667(5)	40.08(2)	20.605(10)	16.692(10)
c (Å)	9.939(4)	26.52(1)	10.002(6)	18.412(10)	15.967(8)
β (deg)		90.08(3)		114.55(4)	
V (Å^3)	10 756	3000	10 976	6197	5418
Z	16	4	16	8	8
μ (cm^{-1})	9.51	8.63	9.46	8.66	9.44
F(000)	4576	1272	4832	2800	2288
D_{calcd} (g cm^{-3})	1.361	1.353	1.421	1.473	1.351
cryst size (mm)	0.3 × 0.4 × 0.4	0.4 × 0.5 × 0.5	0.3 × 0.5 × 0.7	0.4 × 0.5 × 0.6	0.3 × 0.3 × 0.4
2θ range (deg)	5.0−50.0	5.0−55.0	5.0−55.0	5.0−55.0	5.0−55.0
no. of unique rflns	2617	7063	3445	5710	6820
no. of used rflns	2148	4742	2820	2982	3801
no. of variables	245	280	261	316	244
R	0.029	0.042	0.036	0.064	0.044
R_w[a]	0.024	0.034	0.032	0.059	0.033

[a] Weighting scheme $[\sigma(F_o)^2]^{-1}$.

according to the literature method.[9] H_2SiPh_2 and $HSiClPh_2$ were purchased and used as received. IR and NMR spectra (^{1}H, ^{13}C, ^{31}P, and ^{29}Si) were recorded on a JASCO 810 spectrophotometer and on a JEOL EX-400 spectrometer, respectively. Peak positions of ^{31}P{^{1}H} NMR and ^{29}Si{^{1}H} NMR spectra were referenced to external 85% H_3PO_4 and external tetramethylsilane, respectively. Elemental analyses were carried out on a Yanagimoto Type MT-2 CHN autocorder.

Preparation of *mer*-RhCl(H)[SiH(C$_6$H$_4$X-*p*)$_2$] (1, X = H; 2, X = Me; 3, X = OMe; 4, X = F; 5, X = CF$_3$). To a benzene (40 mL) dispersion of $[Rh(PMe_3)_4]Cl$ (1.07 g, 2.4 mmol) was added H_2SiPh_2 (574 mg, 3.1 mmol) in one portion at room temperature. The orange solid dispersed in the solvent gradually turned pale yellow on stirring. After 18 h the resulting solid product was collected by filtration, washed with hexane several times, and dried in vacuo (1.26 g, 96%). Recrystallization from a toluene−hexane mixture afforded **1** as yellow crystals. ^{13}C{^{1}H} NMR (100 MHz in C_6D_6): δ 144.9, 136.1, 19.3 (apparent triplet due to virtual coupling, P(*C*H$_3$)$_3$), 18.1 (d, P(*C*H$_3$)$_3$, *J*(PC) = 20 Hz). Other signals due to phenyl carbons were not observed due to overlapping with the solvent peaks. ^{29}Si{^{1}H} NMR (80 MHz in C_6D_6): δ 14.9 (ddt, *J*(SiRh) = 43 Hz, *J*(SiP(trans to hydride)) = 8 Hz, *J*(SiP(cis to hydride)) = 7 Hz).

Preparation of **2**−**5** was carried out similarly. Complex **2** was recrystallized from a toluene-hexane mixture containing a small amount of PMe_3, while the other complexes were recrystallized from toluene−hexane mixtures.

Measurement of Equilibrium Constants of the Reaction of 1 with Diarylsilanes. A mixture of **1** (9.45 mg, 0.017 mmol), H_2SiPh_2 (6.55 mg, 0.036 mmol), $H_2Si(C_6H_4OMe\text{-}p)_2$ (19.5 mg, 0.080 mmol), and diphenylmethane (internal standard, 3.15 mg) was dissolved in C_6D_6 (0.55 mL). The solution was transferred through a silicon rubber tube into an NMR tube under an Ar atmosphere. After the NMR sample tube was sealed, the ^{1}H NMR peak areas of SiH hydrogens and PMe_3 hydrogens of the complexes were compared with the peak due to the standard at the fixed temperature.

Reaction of D_2SiPh_2 with 3. To an NMR tube (5 mm i.d.) containing **3** (14 mg, 0.023 mmol) C_6D_6 (0.5 mL) was introduced through the rubber septum cap at room temperature. D_2SiPh_2 (4.3 mg, 0.023 mmol) was added to the solution, and then quickly the tube was transferred to the probe of an NMR instrument. The ^{1}H NMR spectrum soon after addition showed the presence of **3**-d_0 and liberated $H_2Si(C_6H_4OMe\text{-}p)_2$ in a 51:49 ratio but did not show the RhH peak of **1** nor the SiH peak of H_2SiPh_2 (or $HDSiPh_2$). Storing the solution for 1 h at room temperature caused the appearance of an ^{1}H NMR peak due to **1** and H_2SiPh_2 (and $HDSiPh_2$).

Thermal Reaction of 1 To Give a Mixture of 6 and 7. A toluene (2 mL) solution of **1** (156 mg, 0.28 mmol) was heated at 110 °C. The pale yellow solution gradually turned brown. After reaction for 90 min the solvent was evaporated to dryness. From the brown residue volatile compounds were removed by a freeze−dry procedure to give a brown powdery product. The ^{1}H NMR analysis of the solid showed the presence of **6** and **7** in an 88:12 ratio. Recrystallization of the product from a toluene−hexane mixture gave **6** as brown crystals (56 mg, 36%). The low isolated yield is partially due to loss during the recrystallization process. ^{13}C{^{1}H} NMR (100 MHz in C_6D_6): δ 150.8 (d, *J* = 9 Hz), 135.5, 127.3, 127.2, 25.6 (dt, P(*C*H$_3$)$_3$ trans to Si, ^1J(CP) = 18 Hz, ^3J(CP) = 3 Hz), 22.7 (dt, P(*C*H$_3$)$_3$ trans to hydride, ^1J(CP) = 13 Hz, ^3J(CP) = 5 Hz). ^{29}Si{^{1}H} NMR (80 MHz in C_6D_6): δ 51.6 (ddt, *J*(SiRh) = 41 Hz, *J*(SiP(trans to Si)) = 198 Hz, *J*(SiP(cis to Si)) = 11 Hz).

Preparation of *mer*-RhCl(H)(SiClPh$_2$)(PMe$_3$)$_3$ (7). To a toluene (30 mL) dispersion of $[Rh(PMe_3)_4]Cl$ (742 mg, 1.7 mmol) was added $HSiClPh_2$ (439 mg, 2.0 mmol) in one portion at room temperature. The orange solid in the reaction mixture gradually turned pale yellow on stirring. After reaction for 72 h the precipitated solid was collected by filtration, washed with hexane repeatedly, and dried in vacuo to give **7** as a pale yellow microcrystalline solid (690 mg, 70%). ^{13}C{^{1}H} NMR (100 MHz in C_6D_6): δ 146.5, 134.7, 130.7, 128.4, 19.0 (apparent triplet due to virtual coupling, P(*C*H$_3$)$_3$), 18.5 (d, P(*C*H$_3$)$_3$, *J*(PC) = 22 Hz). Other signals due to the phenyl carbons are not observed, probably due to overlapping with the solvent peaks. ^{29}Si{^{1}H} NMR (80 MHz in C_6D_6): δ 41.7 (ddt, *J*(SiRh) = 48 Hz, *J*(SiP(cis to hydrido)) = 9 Hz, *J*(SiP(trans to hydrido)) = 15 Hz).

Thermal Reaction of 6. A benzene-d_6 (0.5 mL) solution of **6** (12.4 mg, 0.023 mmol) was transferred to an NMR tube, which was then sealed under Ar. Heating the sample for 24 h at 80 °C results in the appearance of new ^{1}H and ^{31}P{^{1}H} NMR peaks, which are assigned to *cis,mer*-Rh(H)$_2$(SiClPh$_2$)(PMe$_3$)$_3$ (**8**). ^{1}H NMR: δ −9.18 (dddt, *J*(HP) = 179 and 20 Hz, *J*(HRh) = 20 Hz, *J*(HH) = 6 Hz), −18.62 (dddt, *J*(HP) = 18 and 16 Hz, *J*(HRh) = 16 Hz, *J*(HH) = 6 Hz). ^{31}P{^{1}H} NMR: δ −5.92 (dd, *J*(PRh) = 103 Hz, *J*(PP) = 24 Hz), −20.41 (dt, *J*(PRh) = 89 Hz). The molar ratios of **6** and **8** after heating for 24, 48, and 70 h at 80 °C were 60:40, 35:65, and 0:100, respectively.

(9) (a) Price, F. P. *J. Am. Chem. Soc.* **1947**, *69*, 2600. (b) Benkeser, R. A.; Foster, D. J. *J. Am. Chem. Soc.* **1952**, *74*, 5314. (c) Steward, O. W.; Pierce, O. R. *J. Am. Chem. Soc.* **1961**, *83*, 1916. (d) Price, R. T.; Anderson, R. A.; Muetterties, E. L. *J. Organomet. Chem.* **1989**, *376*, 407.

Reaction of 6 with $HSiClPh_2$. A benzene-d_6 (0.5 mL) solution of a mixture of **6** (10.7 mg, 0.019 mmol) and $HSiClPh_2$ (15.9 mg, 0.073 mmol) was transferred to an NMR tube, which was then sealed under Ar. The ^1H and $^{31}P\{^1H\}$ NMR spectra show the presence of **6** and **7** in an 81:19 molar ratio. Heating the sample for 90 min at 80 °C changed the ratio of the complexes to 73:27.

Crystal Structure Determination. Crystals were mounted in a glass capillary tube under argon. The unit cell parameters were obtained by least-squares refinement of 2θ values of 25 reflections with $25° \leq 2\theta \leq 35°$. Intensities were collected on a Rigaku AFC−5R automated four-cycle diffractometer by using graphite-monochromated Mo Kα radiation ($\lambda = 0.710\ 69$ Å) and the $\omega-2\theta$ method. Empirical absorption correction (ψ scan method) of the collected data was applied. Table 5 summarizes crystal data and details of data refinement.

Calculations were carried out by using the program package teXsan on a VAX-II computer. Atomic scattering factors were taken from the literature.[10] A full-matrix least-squares refinement was used for non-hydrogen atoms with anisotropic thermal parameters. Hydrogen atoms, except for the RhH and SiH hydrogens were located by assuming ideal positions ($d = 0.95$ Å) and were included in the structure calculation without further refinement of the parameters. Positions of the RhH and SiH hydrogens were determined by difference Fourier map and were not refined further.

Acknowledgment. This work was financially supported by a Grant-in-Aid for Scientific Research from the Ministry of Education, Science, Sports, and Culture of Japan. T.K. is grateful to the Japan Society for Promotion of Science (JSPS) for a Grant-in-Aid for JSPS fellows.

Supporting Information Available: Tables giving crystallographic data for **1** and **3**−**6** (25 pages). Ordering information is given on any current masthead page.

OM970391Z

(10) *International Tables for X-ray Crystallography;* Kynoch: Birmingham, England, 1974; Vol. IV.